Supplementary Information

Chromosome compartments on the inactive X guide TAD formation independently of transcription during X-reactivation

Bauer *et al.* 2021 Nature Communications

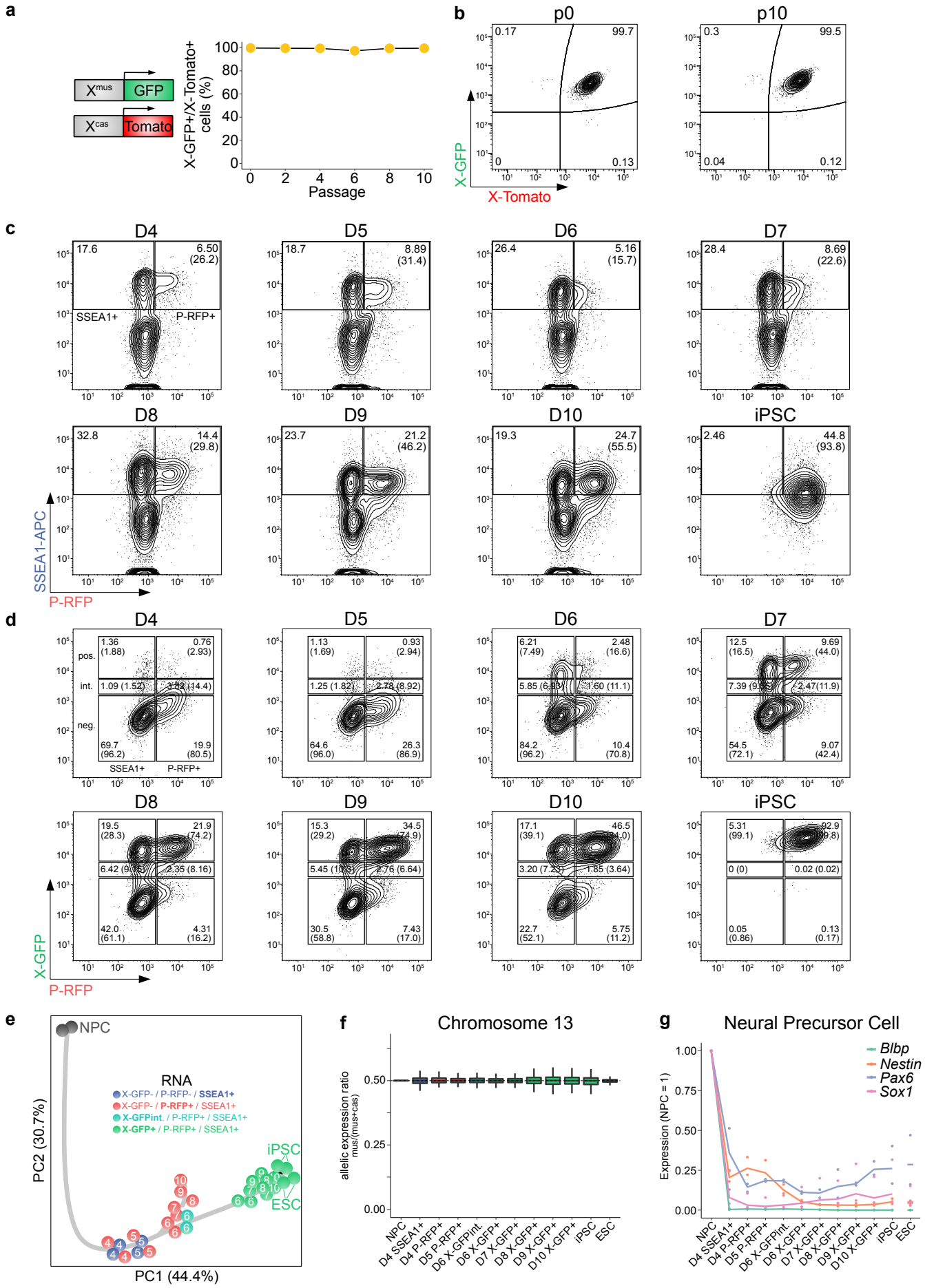

Supplementary Fig. 1 A tailor-made reprogramming system to efficiently trace X-chromosome reactivation.

(legend on next page)

Supplementary Fig. 1 A tailor-made reprogramming system to efficiently trace X-chromosome reactivation. a Left, schematic of the X dual color reporter. Right, quantification of X chromosome loss in X dual color ESCs cultured in serum plus LIF conditions for 10 passages, with passaging every other day. **b** FACS gating strategy of X-GFP and X-Tomato reporter expression at passage 0 and 10. Shown are representative contour plots gated on live cells. Numbers indicate the percentage of cells. **c** FACS gating strategy of SSEA1 and P-RFP reporter expression during a reprogramming time course. Shown are representative contour plots gated on live cells. Numbers indicate the percentage of cells. Numbers in brackets indicate the percentage of P-RFP+ cells out of SSEA1+ cells. **d** FACS gating strategy of P-RFP and X-GFP reporter expression during a reprogramming time course. Shown are representative contour plots gated on SSEA1+ cells in (**c**). Numbers indicate the percentage of cells. **e** PCA of dynamics of gene expression during reprogramming including neural precursor cells (NPCs) (n = 12,318 genes). Solid grey arrow, hypothetical trajectory. Dashed grey arrow, samples deviating from main reprogramming trajectory. **f** Allelic expression ratio (mus/(mus+cas)) of protein-coding genes expressed from chromosome 13 (n = 335). Biallelic expression, ratio = 0.5. Box plots depict the first and third quartiles as the lower and upper bounds of the box, with a band inside the box showing the median value and whiskers representing 1.5x the interquartile range. **g** Average gene expression kinetics of neural precursor cell markers *Blbp*, *Nestin*, *Pax6*, and *Sox1* during reprogramming (n = 2, relative to the levels in NPC).

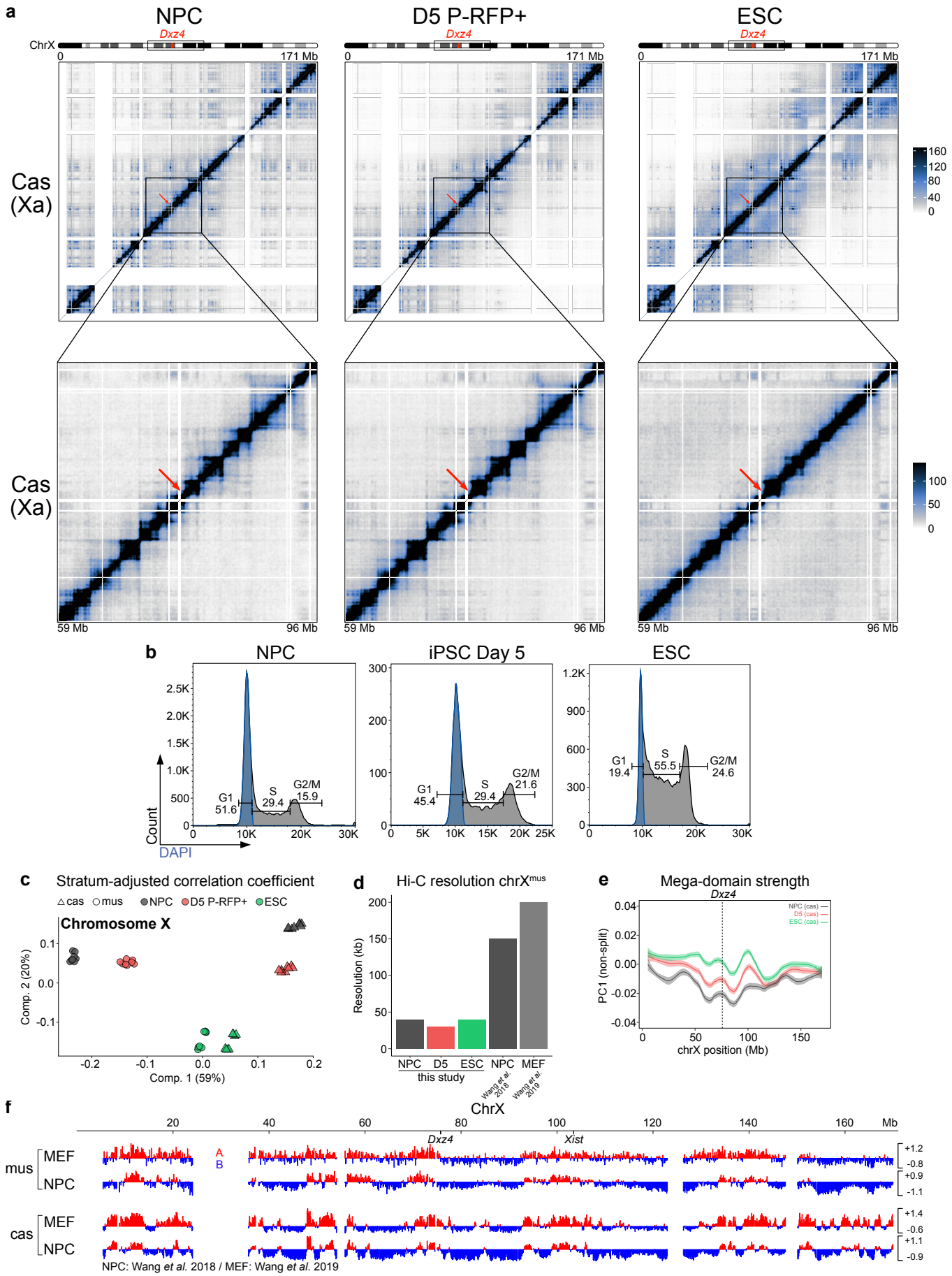

Supplementary Fig. 2 The inactive X chromosome exhibits A/B-like compartmentalization.
(legend on next page)

Supplementary Fig. 2 The inactive X chromosome exhibits A/B-like compartmentalization. **a** Allele-specific Hi-C maps of the always active chromosome X^{cas} across stages. Top: Entire chromosome is shown at 200-kb resolution. Bottom: Zoom-in of the mega-domain boundary is shown at 100-kb resolution. Scale is shown in mega-bases (Mb). The mega-domain boundary *Dxz4* is indicated by a red arrow. White-shaded areas, unmappable regions. **b** FACS analysis of cell cycle using DAPI. Blue shading indicates sorted G1 population. Numbers indicate the percentage of cells. **c** Correlation of Hi-C samples at 100-kb resolution using stratum-adjusted correlation coefficient[1], visualized as a multi-dimensional scaling plot. **d** Hi-C resolution of the inactive chromosome X^{mus} achieved in this study, calculated as described previously[2]. Resolution of comparable studies assessing the inactive X using allele-specific *in situ* Hi-C are shown[3,4]. **e** Mega-domain strength on the active X^{cas} depicted by the PC1 of the Hi-C matrices without splitting at *Dxz4*. Lines show smoothed data from a fitted loess curve with span 0.25. Shading denotes 95% confidence interval. Dotted line indicates position of *Dxz4.* **f** A/B compartments of chromosome X at 100-kb resolution obtained with principal component analysis of matrices split at the *Dxz4* mega-domain boundary of neural precursor cells (NPCs)[3] and mouse embryonic fibroblasts (MEFs)[4]. Positive PC1 values represent A-like compartments (red); negative PC1 values represent B-like compartments (blue).

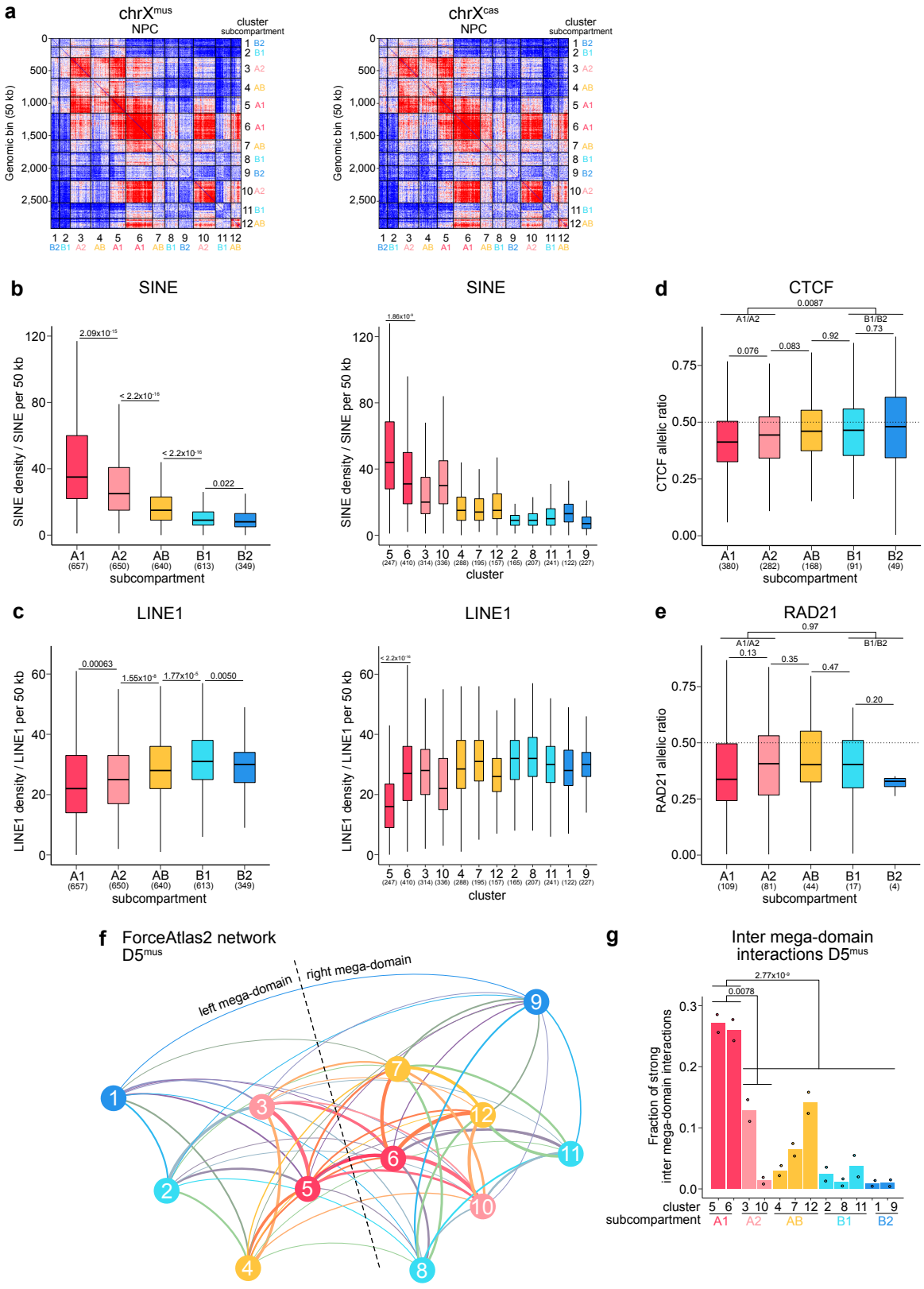

Supplementary Fig. 3 Subcompartmentalization of the inactive X chromosome.
(legend on next page)

Supplementary Fig. 3 Subcompartmentalization of the inactive X chromosome. a Interaction matrices of spatial clusters at 50-kb resolution. **b** Density of SINE repeats per 50 kb bin for subcompartments and spatial clusters. **c** Density of LINE1 repeats per 50 kb bin for subcompartments and spatial clusters. **d** Allelic ratio of CTCF peaks between NPC^{mus} and NPC^{cas} of subcompartments. ChIP-seq data from[3]. **e** Allelic ratio of RAD21 peaks between NPC^{mus} and NPC^{cas} of subcompartments. ChIP-seq data from[3]. (**b**-**e**) The numbers above the bars indicate p-values (two-sample unpaired Wilcoxon-Mann-Whitney test with R defaults). Box plots depict the first and third quartiles as the lower and upper bounds of the box, with a band inside the box showing the median value and whiskers representing 1.5x the interquartile range. n is given in brackets and indicates number of 50 kb bins. **f** Network of spatial clusters on chromosome X^{mus} in D5 P-RFP+ obtained by applying the ForceAtlas2 algorithm to Hi-C interaction patterns of spatial clusters. Each cluster represents a single node of the network. Line-width correlates with interaction strength. **g** Inter-mega-domain interactions of clusters (across the mega-domain boundary) in D5 P-RFP+^{mus}. The numbers above the bars indicate p-values (unpaired two-sided t-test with R defaults). n = 2 biologically independent replicates.

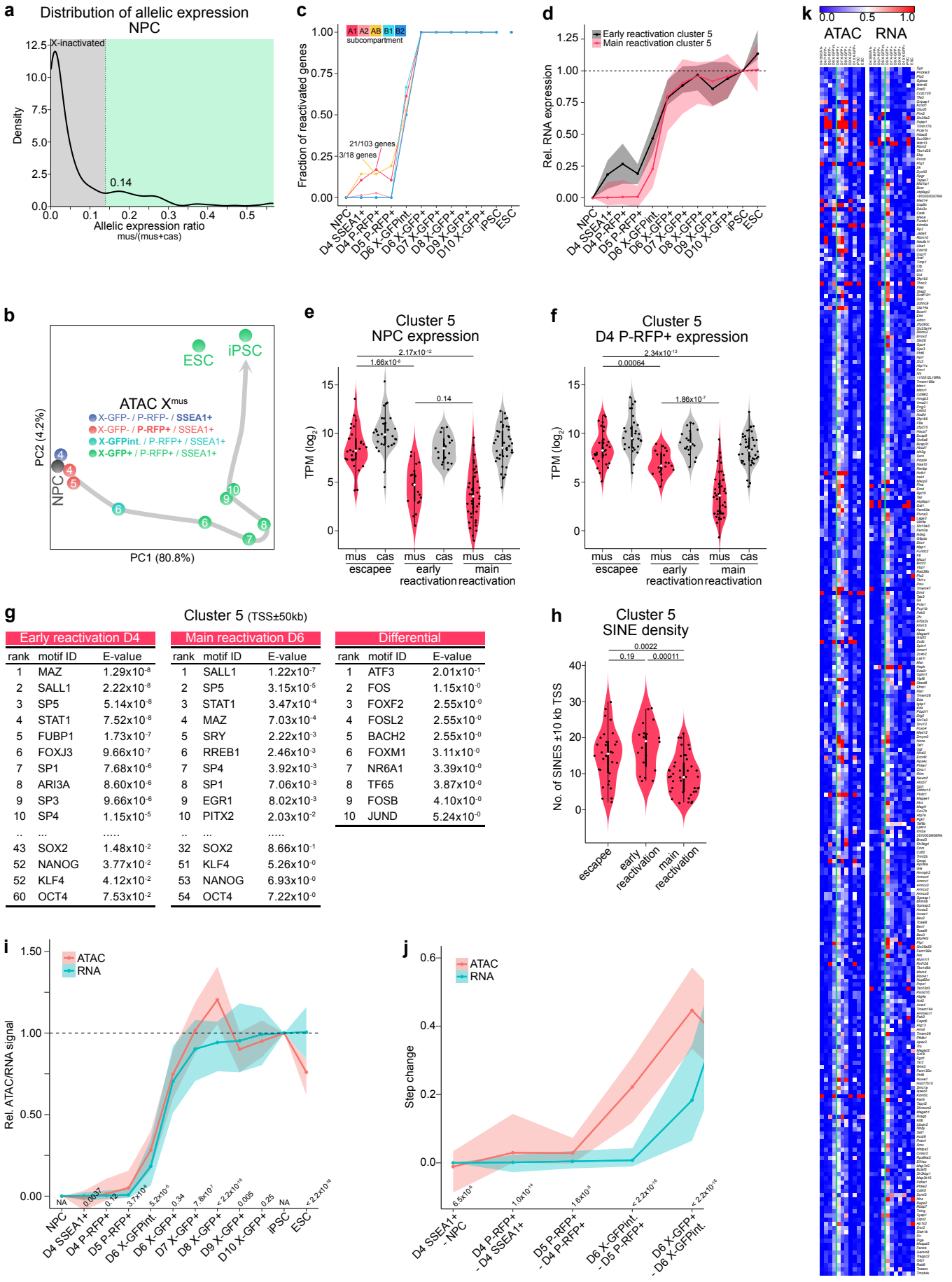

Supplementary Fig. 4 Initiation of chromatin opening and gene expression from a distinct 3D cluster.

(legend on next page)

Supplementary Fig. 4 Initiation of chromatin opening and gene expression from a distinct 3D cluster. a Distribution of the allelic expression ratio of chromosome X in NPCs (n = 275). The dashed line represents the cut-off of 0.14, above which genes were considered biallelically expressed (green shading). Only protein-coding genes with sufficient allelic information, expression for chromosome X^{cas}, and biallelic expression in iPSC and ESC are counted (see methods). **b** PCA of dynamics of chromatin opening on the X^{mus} during reprogramming (n = 570,104 50 kb bins). Grey arrow, hypothetical trajectory. **c** Dynamics of gene reactivation of subcompartments. Fractions of reactivated genes per cluster are shown. 0, no reactivated gene. 1, all genes reactivated. Threshold for gene reactivation, allelic expression ratio >0.14, see (**a**). While subcompartment AB shows a similar fraction of early reactivating genes to A1, it is biased by the low number of genes in this subcompartment, with a total of 18 genes and 3 reactivating at D4 P-RFP+. **d** Relative RNA expression (NPC = 0, iPSC = 1) for genes of cluster 5 reactivating early, at D4 P-RFP+, compared to genes reactivating after that ("main reactivation"). Line shows median. Shading denotes 50% confidence interval. **e** Violin plots showing the RNA expression from the mus allele of genes of cluster 5 in NPCs. TPM, transcripts per million. The numbers above the bars indicate p-values (two-sample unpaired Wilcoxon-Mann-Whitney test with R defaults). **f** As (**e**) in D4 P-RFP+ cells. **g** Enrichment of transcription factor motifs. AME was used to identify differentially enriched motifs from ATAC-seq peaks in a window of +- 50 kb around the TSS of cluster 5 genes reactivating early or after that. Differential AME analysis for early reactivation-specific motifs was performed using peaks around early reactivating genes as primary sequence and peaks around main reactivating genes as control. **h** Violin plots showing the number of SINE repeats in a window of +-10 kb around the TSS of genes of cluster 5. The numbers above the bars indicate p-values (two-sample unpaired Wilcoxon-Mann-Whitney test with R defaults). **i** Relative gene expression and chromatin opening at gene promoters compared (NPC = 0, iPSC = 1). Line shows median. Shading denotes 50% confidence interval. The numbers above the axis indicate p-values (two-sample unpaired Wilcoxon-Mann-Whitney test with R defaults). n = 293. **j** Step changes of gene expression and chromatin opening at gene promoters compared. Line shows median. Shading denotes 50% confidence interval. The numbers above the axis indicate p-values (two-sample unpaired Wilcoxon-Mann-Whitney test with R defaults). n = 293. **k** Step changes of gene expression and chromatin opening at gene promoters compared. Genes are sorted by their chromosomal position. Vertical green line indicates main X-reactivation in the D6 X-GFP+ population. The color gradient represents the step change. Blue, 0. White, 0.5. Red, 1. n = 293.

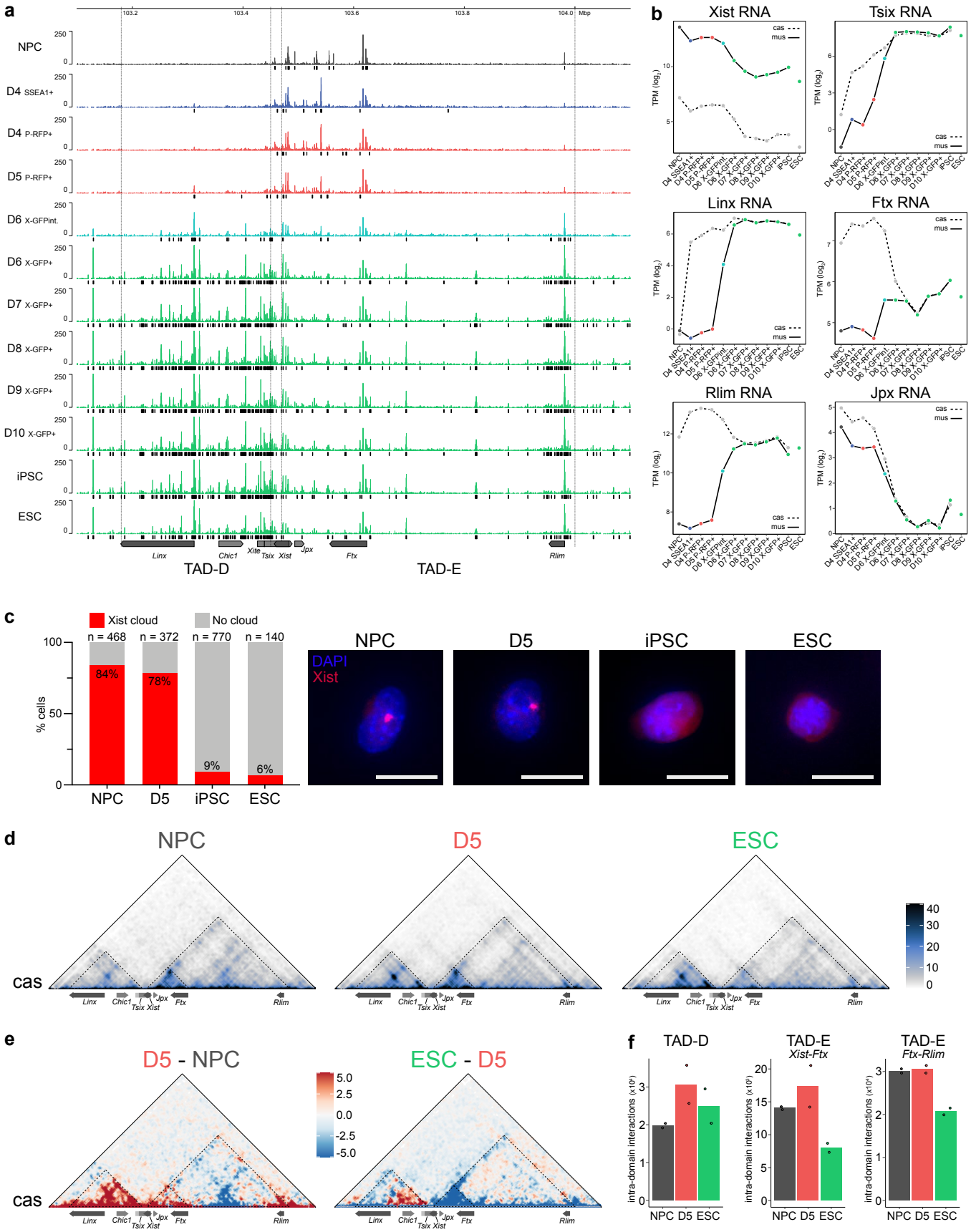

Supplementary Fig. 5 Remodelling of the X-inactivation centre leading to *Xist* downregulation.
(legend on next page)

Supplementary Fig. 5 Remodelling of the X-inactivation centre leading to *Xist* downregulation. **a** ATAC-seq profiles at a region encompassing *Tsix* TAD-D (mm10; 103.18 Mb - 103.45 Mb) and *Xist* TAD-E (mm10; 103.47 Mb - 104.0 Mb). ATAC-peaks in black (except for NPCs, differential peaks compared to NPCs are shown). Only genes with implicated roles in X-inactivation or X-reactivation are shown. **b** RNA expression of *Xist*, *Tsix*, *Linx*, *Ftx*, *Rlim* and *Jpx* (X^{mus} and X^{cas}). **c** Downregulation of Xist RNA during reprogramming based on RNA-FISH. Percentages of cells containing Xist RNA FISH clouds are shown for one of two independent experiments. Scale bar, 5 µm. **d** Allele-specific Hi-C maps of chromosome X^{cas} at 10-kb resolution at a region encompassing TAD-D (left) and TAD-E (right). **e** Differential allele-specific Hi-C maps of chromosome X^{cas} at 10-kb resolution at a region encompassing TAD-D and TAD-E. (**d, e**) Dotted lines show TAD borders and additionally separate TAD-E in two regions at the TSS of *Ftx* (mm10; 103.62 Mb) for quantification in (**f**). **f** Sum of intra-domain interactions of X^{cas} are shown. TAD-E was separated in two regions at the TSS of *Ftx*. n = 2 biologically independent replicates.

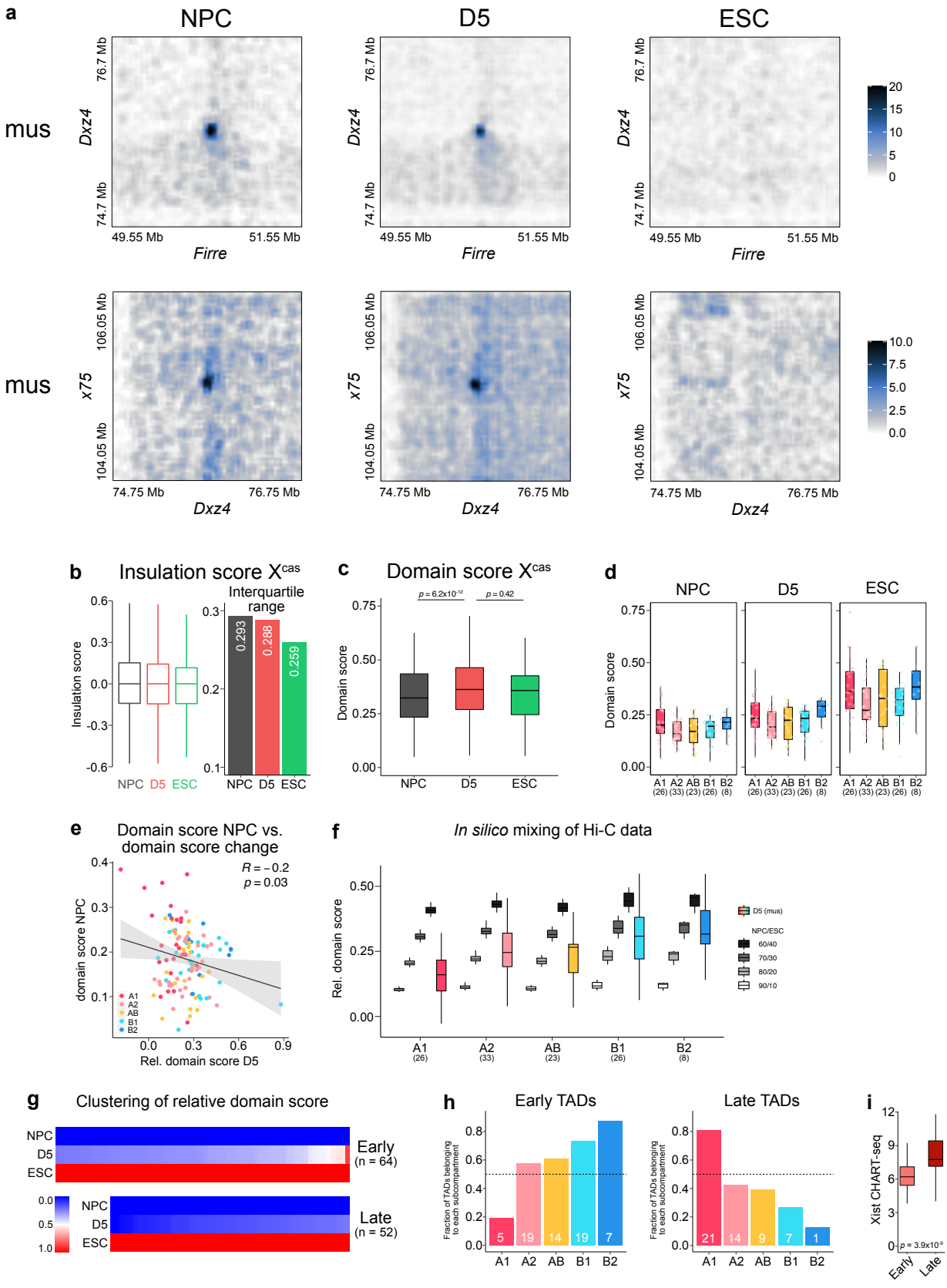

Supplementary Fig. 6 Structural changes during X-reactivation in the absence of chromatin opening and transcription.
(legend on next page)

Supplementary Fig. 6 Structural changes during X-reactivation in the absence of chromatin opening and transcription. a Allele-specific Hi-C maps at 30-kb resolution showing superloop interactions between *Dxz4* and *Firre*, as well as *x75* and *Dxz4* ± 1 Mb. **b** Comparison of insulation scores for chromosome X^{cas}. Interquartile range of insulation scores is shown on the right. n = 2,785 50 kb bins. **c** Comparison of domain scores for chromosome X^{cas}. The numbers above the bars indicate p-values (two-sample unpaired Wilcoxon-Mann-Whitney test with R defaults). n = 100 TADs. **d** Domain scores for X^{mus} of subcompartments. n is given in brackets and indicates number of TADs. **e** Correlation between the absolute domain score in NPCs and the relative domain score at D5 is shown. Points represent TADs. Colours of points indicate subcompartments. R and p-values calculated by Pearson's correlation are shown. Black line represents linear regression fitting. Shading denotes 95% confidence interval of the fit. **f** relative domain score is shown for *in silico* mixed Hi-C matrices of NPC^{mus} with ESC^{mus} at given ratios and compared to the relative domain score of $D5^{mus}$. n is given in brackets and indicates number of TADs. **g** *k*-means clustering (*k* = 2) of relative domain scores to identify early and late TADs. **h** Comparison of the fraction of TADs of each subcompartment belonging to early or late TADs. Absolute numbers of TADs for each subcompartment are given in the barplots. **i** Xist RNA enrichment of early and late TADs in NPCs (composite scaled data). CHART-seq data from[3]. The numbers above the bars indicate p-values (two-sample unpaired Wilcoxon-Mann-Whitney test with R defaults). n = 64 early TAD and 52 late TADs. (**b,c**,**d**,**f**,**i**) Box plots depict the first and third quartiles as the lower and upper bounds of the box, with a band inside the box showing the median value and whiskers representing 1.5x the interquartile range.

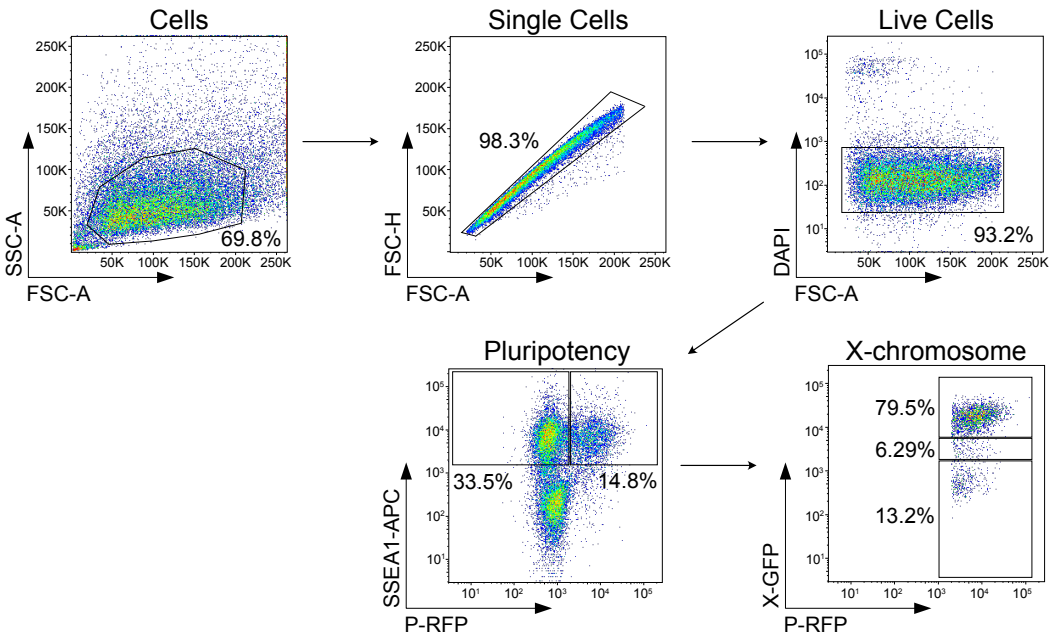

Supplementary Fig. 7 FACS gating strategy. The gating was performed as follows, exemplified for day 8 iPSCs: First, forward and side scatter were used to gate out debris. Second, forward scatter height and area were used to gate out doublets. Third, DAPI-positivity was used to gate out dead cells. Fourth, pluripotent cells were then defined on live cells by SSEA1-APC+ or SSEA1-APC+/P-RFP+. Last, on pluripotent cells, cells corresponding to different X-status were defined using X-GFP. Boundaries between pluripotent and non-pluripotent populations, as well as between X-reactivated and non-reactivated populations were defined using non stained cells and cell lines without fluorescent reporters as negative controls.

Supplementary Table 1. Number of normalized allelic reads of each *in situ* Hi-C dataset generated in this study.

sample	replicate	chr X (mus)	chr X (cas)	chr 13 (mus)	chr 13 (cas)
NPC	1	6,087,754	7,498,096	10,774,993	10,618,036
NPC	2	3,043,877	3,749,048	14,484,897	14,364,026
D5 P-RFP+	1	12,143,539	9,244,472	13,843,684	13,408,834
D5 P-RFP+	2	6,071,770	4,622,236	6,921,842	20,098,602
ESC	1	10,432,393	10,163,224	10,774,993	10,618,036
ESC	2	5,216,196	5,081,612	14,484,897	14,364,026

Supplementary Table 2 List of primers used in this study.

Sequence	Target gene/region	Orientation	Application
ATGAATACGGCTACAGCAACAGG	*Gapdh*	Forward	quantitative RT-PCR
CTCTTGCTCAGTGTCCTTGCTG	*Gapdh*	Reverse	quantitative RT-PCR
AGGAAACGACGAGAACAGTTGA	MKOS cMyc-Klf4	Forward	quantitative RT-PCR
GACGCAGTGTCTTCTCCCTTC	MKOS cMyc-Klf4	Reverse	quantitative RT-PCR
GGACCACCTTGCCTTACACAT	MKOS Klf4-Oct4	Forward	quantitative RT-PCR
GAAGCTTAGCCAGGTTCGAGA	MKOS Klf4-Oct4	Reverse	quantitative RT-PCR
ACCACACTCTACTCAGTCCCT	MKOS Oct4-Sox2	Forward	quantitative RT-PCR
AGCTCCGTCTCCATCATGTT	MKOS Oct4-Sox2	Reverse	quantitative RT-PCR
CTACCACCGATTCTATGCCCC	rtTA	Forward	quantitative RT-PCR
CGCTTTCGCACTTTAGCTGTT	rtTA	Reverse	quantitative RT-PCR
TTAGCCAGGCAGCTAGAGGA	*Jpx*	Forward	quantitative RT-PCR
AGCCGTATTCCTCCATGGTT	*Jpx*	Reverse	quantitative RT-PCR
ATCATACTAAAGGCCACACAAAGAAT	*Xist* (mus)	Forward	quantitative RT-PCR
ATTTGGATTGCAAGGTGGAT	*Xist* (mus)	Reverse	quantitative RT-PCR

Supplementary References

1. Yang, T. *et al.* HiCRep: assessing the reproducibility of Hi-C data using a stratum-adjusted correlation coefficient. *Genome Res.* **27**, 1939–1949 (2017).
2. Rao, S. S. P. *et al.* A 3D map of the human genome at kilobase resolution reveals principles of chromatin looping. *Cell* **159**, 1665–1680 (2014).
3. Wang, C.-Y., Jégu, T., Chu, H.-P., Oh, H. J. & Lee, J. T. SMCHD1 Merges Chromosome Compartments and Assists Formation of Super-Structures on the Inactive X. *Cell* vol. 174 406–421.e25 (2018).
4. Wang, C.-Y., Colognori, D., Sunwoo, H., Wang, D. & Lee, J. T. PRC1 collaborates with SMCHD1 to fold the X-chromosome and spread Xist RNA between chromosome compartments. *Nat. Commun.* **10**, 2950 (2019).